Glacial-interglacial size variability in the diatom *Fragilariopsis kerguelensis*: Possible iron/dust controls?

G. Cortese,[1] R. Gersonde,[2] K. Maschner,[3] and P. Medley[4]

Received 16 June 2011; revised 6 December 2011; accepted 7 December 2011; published 16 February 2012.

[1] The valve area of *Fragilariopsis kerguelensis*, the most abundant diatom species in the Southern Ocean, strongly changes in size in response to varying conditions in the surface ocean. We examined the link, both in two iron fertilization experiments and in sediment samples covering several glacial Terminations, between size variability in this species and environmental conditions across the Antarctic Polar Front, including sea ice extent, sea surface temperature, and the input of eolian dust. The iron fertilization experiments show valve area to be positively correlated with iron concentrations in ambient waters, which suggests the possibility of a causal relation between valve size of *Fragilariopsis kerguelensis* and ambient surface water iron concentration. Larger valves are usually found during glacial times and thus seem to be related to lower sea surface temperature and wider sea ice coverage. Moreover, our results indicate that there usually is a strong correlation between larger valve size and increased input of eolian dust to the Southern Ocean. However, this correlation, obvious for the fertilization experiments and for glacial Terminations I, II, III, and V, does not seem to be valid for Termination VI, where size appears to be inversely correlated to dust input.

Citation: Cortese, G., R. Gersonde, K. Maschner, and P. Medley (2012), Glacial-interglacial size variability in the diatom *Fragilariopsis kerguelensis*: Possible iron/dust controls?, *Paleoceanography*, *27*, PA1208, doi:10.1029/2011PA002187.

1. Introduction

[2] The export of carbon dioxide from the atmosphere toward the deep ocean represents a sink for atmospheric carbon dioxide, and this export process is referred to as the "biological pump" [*Falkowski et al.*, 1998]. This pump is controlled by changes in the primary productivity and export efficiency of the organisms living at the surface of the ocean. Past changes in the efficiency of the biological pump during glacial and interglacial times could have directly affected the atmospheric carbon dioxide content.

[3] In high-nutrient, low-chlorophyll areas (HNLC) of the ocean, phytoplankton does not completely utilize available nutrients, and high levels of macronutrient (e.g., nitrogen and phosphorus) correspond to lower than expected primary production. This puzzling observation was explained in terms of productivity limitation due to lack of the micronutrient iron in the upper water column [*Martin and Fitzwater*, 1988; *Martin et al.*, 1990]. As a corollary of this, *Martin et al.* [1990] hypothesized that large blooms of phytoplankton could be stimulated by adding iron into HNLC areas, increasing the efficiency of the biological pump and resulting in a net sequestration of carbon dioxide from the atmosphere.

[4] Large-scale additions of dissolved iron to HNLC areas (iron fertilization experiments) have been performed extensively during the last two decades at a variety of locations [e.g., *Martin and Fitzwater*, 1988; *de Baar et al.*, 1990; *Martin et al.*, 1994; *Coale et al.*, 1996; *Boyd et al.*, 2000]. These iron fertilization experiments, along with a series of in vitro experiments [*Hutchins and Bruland*, 1998; *Takeda*, 1998; *De La Rocha et al.*, 2000; *Timmermans et al.*, 2004] have demonstrated how iron limitation strongly influences the relative uptake ratios of the main nutrients in diatoms, and thus relief from iron limitation may have a strong imprint on the biogeochemical cycle of these nutrients. In particular, the most common large, bloom-forming diatoms in the Southern Ocean (*Fragilariopsis kerguelensis*, *Actinocyclus* sp., *Thalassiosira* sp.) display a marked decrease in the silicate/nitrate depletion ratio with increased iron availability [*Timmermans et al.*, 2004]. This is a result of a decrease of silicate (and concomitant increase in nitrate) consumption in response to increasing dissolved iron concentration [*De La Rocha et al.*, 2000; *Timmermans et al.*, 2004].

[5] Interestingly, such a relief from iron limitation has large consequences on the export of dissolved nutrients from the Southern Ocean toward lower latitudes [*Sarmiento et al.*, 2004]. In fact, the modern Southern Ocean is iron limited (higher silicate/lower nitrate consumption) and thus exports nitrate toward lower latitudes via Sub-Antarctic Mode Water (SAMW). When the Southern Ocean is under iron-replete conditions (lower silicate/higher nitrate consumption) it

[1]Department of Paleontology, GNS Science, Lower Hutt, New Zealand.
[2]Geosciences Division, Alfred Wegener Institute for Polar and Marine Research, Bremerhaven, Germany.
[3]German Oceanographic Museum, Stralsund, Germany.
[4]Cooperative Institute for Research in Environmental Science, University of Colorado at Boulder, Boulder, Colorado, USA.

0883-8305/12/2011PA002187

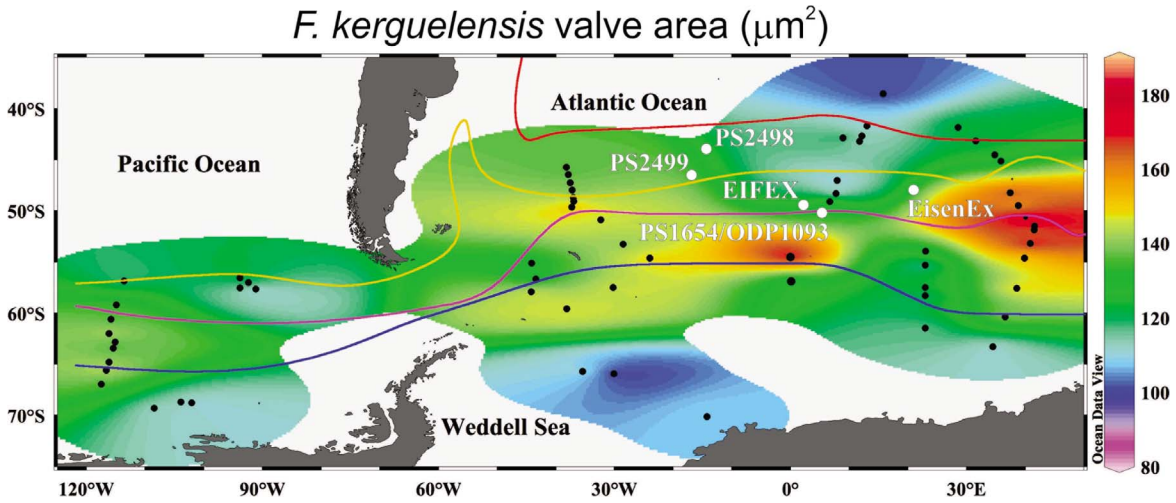

Figure 1. Location of the studied sediment cores and iron fertilization experiments. The background map represents the modern average valve area in *Fragilariopsis kerguelensis* (reprinted from *Cortese and Gersonde* [2007], with permission from Elsevier). The black dots are the surface sediment samples used to produce the map, and oceanic frontal positions and maximum sea ice extent are according to *Belkin and Gordon* [1996]: Subtropical Front (red), Sub-Antarctic Front (yellow), Antarctic Polar Front (purple), winter sea ice edge (blue).

exports silicate, thus strongly affecting ecosystem functioning at a global level [*Sarmiento et al.*, 2004].

[6] An interesting aspect of iron-limited diatom blooms is its connection to the observation that iron limitation is relieved in the Southern Ocean during glacial times, due to increased levels of iron in the surface waters. The main sources of iron to the surface ocean are assumed to be eolian dust, upwelling, and melting icebergs. *Martínez-Garcia et al.* [2009] recently demonstrated how iron fertilization has been a recurrent feature of the sub-Antarctic region over last 1.1 Ma, as dust/iron inputs to the ocean and marine export production records are closely correlated over the entire interval.

[7] The European Project for Ice Coring in Antarctica (EPICA) recovered an ice core that provides a climate record for the past 800,000 years [*EPICA Community Members*, 2004; *Jouzel et al.*, 2007]. We will use the dust record from this core as a proxy for dust deposition into the Southern Ocean, following John Martin's iron fertilization hypothesis and assuming that the fertilization during glacial periods mainly occurs through dust-borne iron [*Martin et al.*, 1990].

[8] The Southern Ocean is the largest HNLC area of the world, and here marine diatoms are the main primary producer and exporter of organic carbon. In the Southern Ocean, the dominant diatom species *Fragilariopsis kerguelensis* displays a strong variability in size [*Cortese and Gersonde*, 2007], but the specific environmental controls for this variability are currently unknown.

[9] The present study is aimed at testing whether the observed pattern of larger *F. kerguelensis* during glacial times, and smaller *F. kerguelensis* during interglacial times at Termination I [*Cortese and Gersonde*, 2007] also holds true for older Terminations. We additionally want to investigate the link between size changes in this diatom and several proxy records including summer sea surface temperature (SST), sea ice extent, major community shifts within diatoms, and eolian input. Under perturbed modern conditions, we also analyze the size variability of this species during two artificial iron fertilization experiments in the Southern Ocean: EIFEX [*Smetacek et al.*, 2005] and EisenEx [*Smetacek*, 2001].

2. Material and Methods

[10] We analyzed microscopic slides prepared from water samples collected during two iron fertilization experiments (Figure 1 and auxiliary material Data Set S1): the EIFEX iron fertilization experiment, conducted at the Antarctic Polar Front (49.4°S, 2.25°E) during R/V "Polarstern" expedition ANTXXI/3 [*Smetacek et al.*, 2005], and the EisenEx fertilization experiment, that took place at 48°S, 21°E during expedition ANTXVIII/2 [*Smetacek*, 2001].[1]

[11] Sediment samples covering the last glacial Termination (Figure 1 and Data Set S2) were analyzed from R/V "Polarstern" cores PS1654 (50.2°S, 5.7°E, Antarctic Polar Front), PS2498 (44.2°S, 14.2°W, north of Subantarctic Front), and PS2499 (46.5°S, 15.3°W, Subantarctic Front). Additional sediment samples (Data Set S3) were obtained from Ocean Drilling Program (ODP) Site 1093, cored in the southeast Atlantic sector of the Southern Ocean during Leg 177, close to the position of piston core PS1654 [*Hodell et al.*, 2002]. This site is located at the Antarctic Polar Front and the examined sediment core documents the last 7 glacial cycles (ca. 600,000 years).

[12] The age model for ODP Site 1093 has been developed using the software Analyseries [*Paillard et al.*, 1996] to match the diatom-derived SST record from this site [*Schneider-Mor et al.*, 2008] and the EPICA ice core temperature record

[1]Auxiliary material data sets are available at ftp://ftp.agu.org/apend/pa/2011pa002187. Other auxiliary material files are in the HTML.

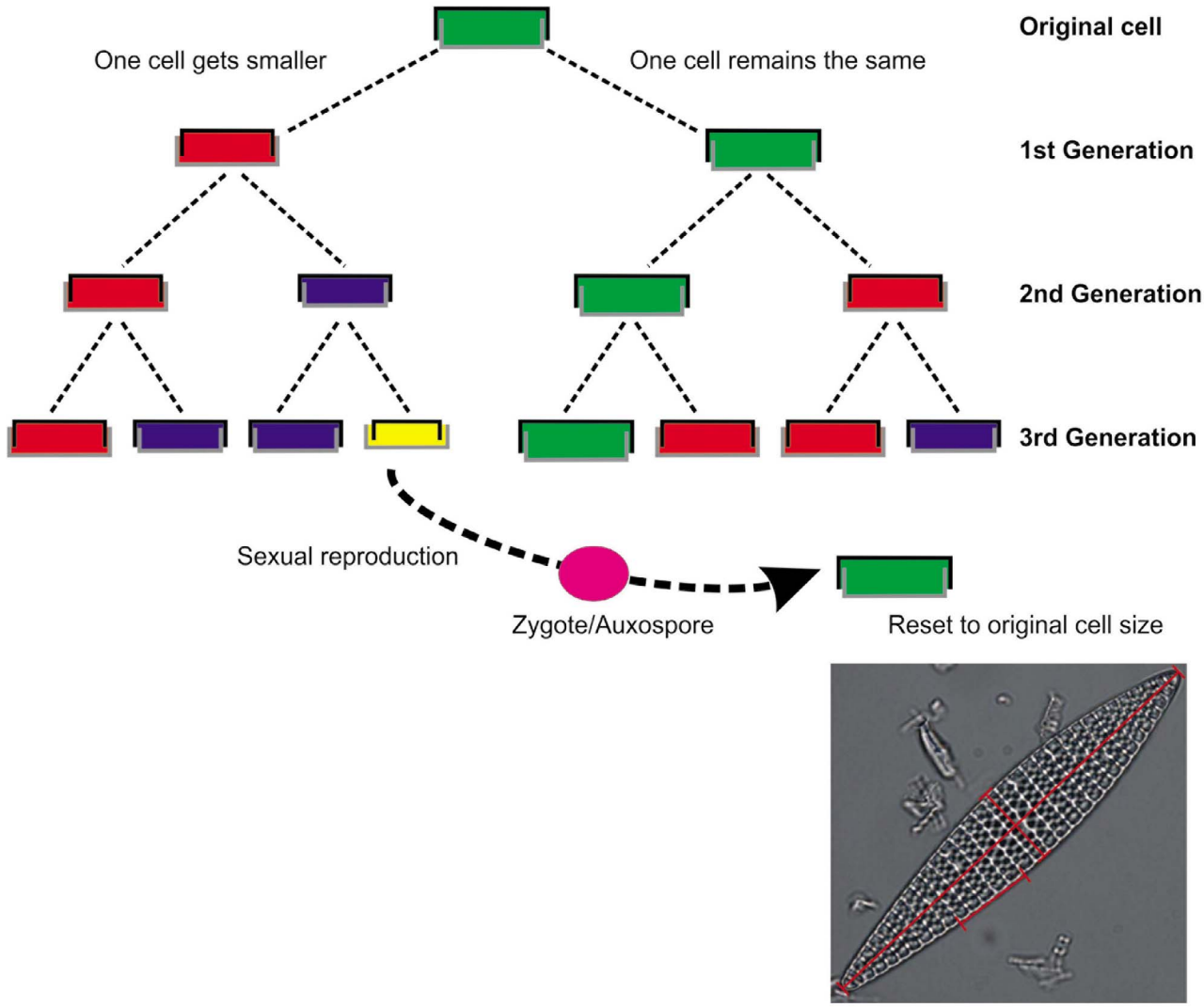

Figure 2. Schematic representation of a diatom's life cycle. The number of generations involving asexual reproduction is not limited to three, and the switch to sexual reproduction involves the release of gametes, formation of a zygote, and resetting of the valve size to the maximum one. The image at the bottom is a valve of *F. kerguelensis*, with the main measurements taken in this study shown as red bars.

[*Jouzel et al.*, 2007] plotted on its EDC3 chronology [*Parrenin et al.*, 2007]. The diatom-derived SST data for ODP Site 1093 are reported in Data Set S5.

[13] The cleaning of the sediment samples and the preparation of permanent slides for light microscopy followed a routine method established at the Alfred Wegener Institute for Polar and Marine Research (AWI), described by *Gersonde and Zielinski* [2000]. Pictures and measurements of the diatom species *Fragilariopsis kerguelensis* were taken following a method described by *Cortese and Gersonde* [2007]. An average of 40.5 specimens for each of the 206 samples (8343 pictures in total) has been photographed using a video camera attached to a Zeiss Axioskop microscope, at 1000x magnification. The public domain image analysis software "ImageJ" (freely available from the National Institute of Health Webpage: http://rsb.info.nih.gov) has been used to measure the length and width of the specimen, and the length of five costae within it (see Figure 2, image at bottom).

[14] Measurements of iron and dust concentrations/fluxes from the EPICA Dome C core are from *EPICA Community Members* [2004], *Wolff et al.* [2006], and *Lambert et al.* [2008]. The reader is referred to these papers for details on the analytical techniques used. Fe fluxes from the EPICA Dome C core are reported in Data Sets S4 and S5. The data pertaining to the EPICA ice core have been plotted on its EDC3 chronology [*Parrenin et al.*, 2007].

[15] MATLAB® was used to perform various statistical tests: statistical power, chi-square, two-sample Kolmogorov-Smirnov, and Wilcoxon rank sum test.

[16] The statistical power test was used to evaluate whether forty diatom specimens were a large enough sample size to capture the variability in the real population and justify the inferences made in this paper. A chi-square test was used to assess whether valve area data were normally distributed, and two-sample Kolmogorov-Smirnov and Wilcoxon rank

sum tests were used to check whether glacial and interglacial valve areas were significantly different.

[17] A sample size of 40 measured specimens proved to be adequate to be able to separate, at power 0.90 and via a *t* test, between a sample from a glacial interval and one from an interglacial interval, and vice versa.

[18] As the chi-square tests indicated that most of the tested populations had nonnormal distributions, the further tests we used to evaluate significant differences in our data sets were nonparametric.

[19] Both the two-sample Kolmogorov-Smirnov and Wilcoxon rank sum test confirmed how the valve area values measured in samples coming from glacial and interglacial intervals are significantly different, both within the same core (tested for PS2498, PS2499, PS1654) and for the whole Termination I data set.

[20] More detailed explanations of statistical testing are available in Texts S1 and S2, while Figures S1 and S2 provide error bar graphs (age versus area with standard deviation for each data point) for all the valve area records.

3. Diatom Life Cycle

[21] Diatoms (microscopic algae belonging to the Class Bacillariophyceae) require sunlight to photosynthesize, limiting their distribution to the uppermost 200 m of the water column. They are especially abundant in the ocean, where they are estimated to contribute up to 45% of the total oceanic primary production [*Mann*, 1999]. The hallmark of diatoms is their pillbox shaped cell wall made of silica ($SiO_2 \times nH_2O$), which can be preserved in the sedimentary record.

[22] The abundance of diatoms varies in space and time as a response to environmental variables and availability of macronutrients (nitrate, phosphate) and micronutrients (iron). Some of these nutrients may at times not be available in high enough levels, and thus become limiting for diatom growth and bloom formation. During such blooms, diatoms rapidly increase their numbers by repeatedly undergoing vegetative (asexual/mitotic) reproduction by cell fission. Diatoms are characterized by a peculiar structure and division modality. The pillbox shaped cell wall is constituted by two valves, the bottom valve (hypotheca) is slightly smaller than the upper one (epitheca). When a cell undergoes division, each daughter cell always builds a new hypotheca. It follows that one of the two daughter cells will end up being slightly smaller than its parent (Figure 2) and, through successive divisions, the average size of diatom cells in a population will decrease. This process can be compensated by the formation of new large cells that occurs during sexual reproduction. The sexual phase can be induced in cells that have reached a species-specific threshold size and includes the formation of gametes, their fusion, and formation of a zygote (auxospore) within which cells of the maximum size are produced [*Chepurnov et al.*, 2004]. Such a switch to a sexual phase has been demonstrated to occur, with the formation of auxospores, in *F. kerguelensis* during an iron-induced bloom in the Southern Ocean [*Assmy et al.*, 2006]. We therefore expect larger spores upon relief from iron limitation.

[23] In sediment samples, many successive generations/blooms of diatom valves are accumulated in the same layer. As such, the average valve size of a population will represent an integrated record of several bloom seasons and the frequency at which sexual reproduction was induced over a time interval of possibly several hundred years, rather than reflecting the dynamics of a single bloom episode. Nonetheless, the sedimentary record of diatom size variability seems to suggest that size in some diatom species might be strongly related to specific environmental conditions.

[24] Valves of *F. kerguelensis* range generally from 10 to 75 μm in length, and 5 to 11 μm in width. The valves have an elliptical to lanceolate shape, and are isopolar (i.e., the two extremes, poles, are identical, and the valve is symmetrical along the transversal axis). Four to seven costae are present over 10 μm, and two rows of alternating pores, easily resolved under light microscopy, are present between two adjacent costae. The length of five costae (Figure 2) were recorded to allow comparisons to the results of *Fenner et al.* [1976], who first investigated *F. kerguelensis* size variability in the South Pacific Ocean.

4. Results

4.1. Fertilization Experiments

[25] In order to test how iron availability might affect size in *Fragilariopsis kerguelensis*, we analyzed several samples collected during two iron fertilization experiments (Figure 1) conducted at the Antarctic Polar Front in the Atlantic Sector of the Southern Ocean (EIFEX [*Smetacek et al.*, 2005] and EisenEx [*Smetacek*, 2001]). During these experiments, a suitable oceanic eddy in a high-nutrient, low-chlorophyll area is identified and tracked with an inert tracer (usually SF_6, sulphur hexafluoride), while at the same time being fertilized with several tons of dissolved iron. Time series for many biological and geochemical indicators are then generated for the few weeks following the fertilization, in order to document the occurrence and characteristics of the ensuing plankton bloom. We studied changes in average valve sizes both inside the fertilized patch, and in a few additional control samples outside it, for both the EIFEX and EisenEx fertilization experiments. The average valve size of *Fragilariopsis kerguelensis* is smaller in the outside patch compared to the fertilized patch throughout the EIFEX iron fertilization experiment (Figure 3). Inside the fertilized patch, the size remains at around 160 μm^2 during the first 8 days of the experiment, then drops to ca. 125 μm^2, and displays a steady rising trend after ca. 12 days, with a maximum size of 210 μm^2 at about 36 days from the start of the experiment. The four control samples from outside the fertilized patch display an offset of ca. 30 μm^2 compared to the in-patch samples, and the size increases only slightly after ca. 17 days from the beginning of the fertilization. However, average valve size is greater in patch even before the fertilization occurs, and throughout the experiment. The similar increasing trends from day 18 to 33 both in and out of patch suggest that the response in patch is mirrored by a similar response outside of the fertilized patch.

[26] With the exception of one sample, the size of *F. kerguelensis* is larger in the in patch, compared to the out patch samples during the EisenEx experiment as well, and the offset between the two curves is ca. 20 μm^2. Although there is a slight trend toward larger sizes as the experiment progressed, the last analyzed sample (ca. 155 μm^2 at 21 days from start of the experiment) most likely does not capture the

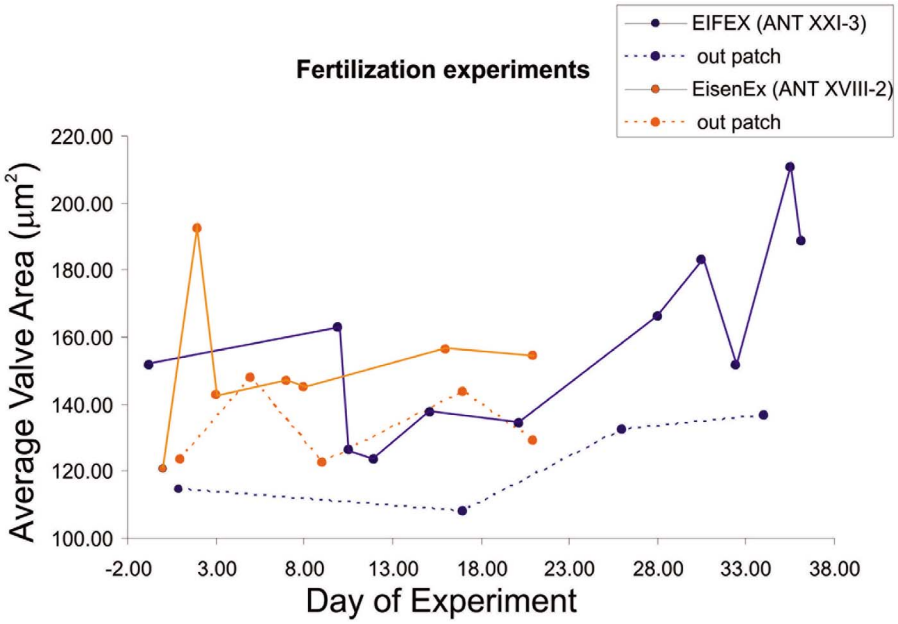

Figure 3. *F. kerguelensis* valve area through two iron fertilization experiments. Samples from EIFEX [*Smetacek et al.*, 2005] and EisenEx [*Smetacek*, 2001]. The solid lines represent samples from within the fertilized patch, while the dotted lines refer to the out-patch, control samples.

rapid increase in size observed during the second half of the EIFEX experiment. A very rapid increase is observed, for a single sample, two days after the start of the experiment.

4.2. Last Glacial Termination (Termination I)

[27] The valve size evolution through the last 35 ka (Figure 4) is remarkably similar for the three examined locations, two of which are from north of the Sub-Antarctic Front (PS2498 and PS2499), while the remaining one (PS1654) has been sampled at the Antarctic Polar Front in the Atlantic Sector of the Southern Ocean (Figure 1). All three cores have substantially larger valves during glacial compared to interglacial times. Average valve sizes oscillate around 190–210 μm^2 during the interval 35 to 17–18 kyr, then rapidly decrease throughout the glacial Termination, and stabilize to their smaller interglacial sizes after ca. 8 kyr BP. The only two noticeable differences among the core sites are the following:

[28] 1. The Antarctic Polar Front location (core PS1654) seems to document larger valve size during the Holocene (140–150 μm^2) compared to the 100–110 μm^2 observed at the two sub-Antarctic sites (PS2498 and PS2499).

[29] 2. At the Sub-Antarctic Front location (core PS2499), average valve size at the start of glacial Termination (220 μm^2 at 18 ka) is much larger than at the other two core sites.

[30] Dust flux values for the Epica Dome C (EDC) ice core are much higher during glacial than interglacial times: the main decrease occurs at ca. 19–16 kyr (and is thus synchronous to the decrease in valve area), after which dust flux values are very low.

4.3. Previous Terminations

[31] The analyzed sediment samples from ODP Site 1093 (Antarctic Polar Front) cover the last 550 kyr, including the four transitions from glacial to interglacial conditions that we analyzed (Terminations II, III, V, and VI). We were particularly interested in examining changes in average valve size of *F. kerguelensis* during glacial, interglacial, and glacial Termination conditions, and their link to several environmental proxy records including sea surface temperature, sea ice extent, major ecosystem shifts within diatoms, and eolian dust/Fe flux input (Figures 5 and 6).

4.3.1. Termination II

[32] At ODP Site 1093, SST [*Schneider-Mor et al.*, 2008] is much colder under full glacial conditions (Marine Isotope Stage, MIS 6) than during the following full interglacial (MIS 5). This is marked with a sharp transition (Figure 5), with SST rising from ca. 0.5°C to an interglacial maximum of ca. 5°C. Following an interglacial optimum, SST slightly decreases and fluctuates around 3.5°C. There is a clear correlation between SST and relative abundances of the *Fragilariopsis curta* group, a proxy for winter sea ice (Figure 5): during full glacial times, when SST is low, *F. curta* is constantly abundant and reaches its peak right before the start of Termination II. With the onset of the transition, the abundance of this species drops to about zero, indicating how there is almost no sea ice present during interglacial times. *F. kerguelensis* is abundant during the whole period, with a slight increase during warmer interglacial times (Figure 5). Shortly before and during Termination II, this species shows a sharp shift in size (Figure 6), as its average valve area switches from high values during glacial times (ca. 200 μm^2) to much lower values during interglacial intervals (ca. 100 μm^2). Termination II shows a drop to the lowest observed average area values (ca. 70 μm^2). A positive correlation is apparent between iron input and average area (Figure 6), as during full glacial times iron is high and constantly available for *F. kerguelensis* and valve areas are around 200 μm^2. As iron decreases during Termination II,

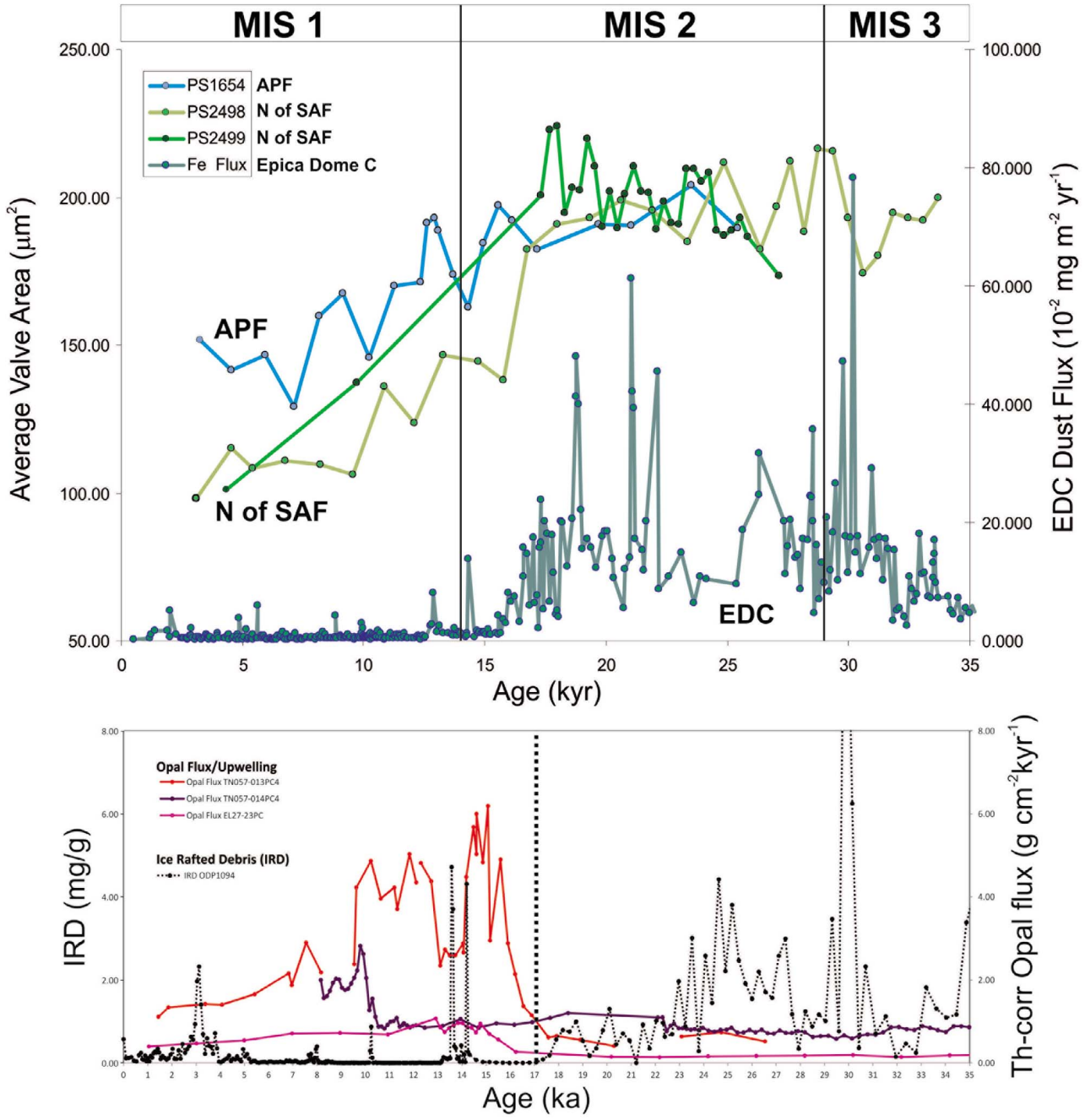

Figure 4. (top) *F. kerguelensis* valve area and dust flux at EPICA Dome C. The Marine Isotope Stage (MIS) boundaries are after *Lisiecki and Raymo* [2005], while the iron flux data are from *Lambert et al.* [2008] and are also reported in Data Set S4. (bottom) IRD record from ODP Site 1094 and Th-corrected opal flux data during Termination I. The ice-rafted debris record from IODP Site 1094 [*Kanfoush et al.*, 2002] appear as a dotted black line, and the Th-corrected opal flux data [*Anderson et al.*, 2009] from cores TN057–013PC4, TN057–014PC4, and EL27–23PC are shown in shades of red. The right-hand scale applies to both IRD (in mg/g) and Th-corrected opal flux (in g cm^{-2} kyr^{-1}). The vertical dashed line at 17 ka roughly marks the start of the glacial Termination, with a sharp decrease in valve size coinciding with the shift from (larger) predominantly eolian/IRD to (smaller) upwelling/iceberg sources of iron.

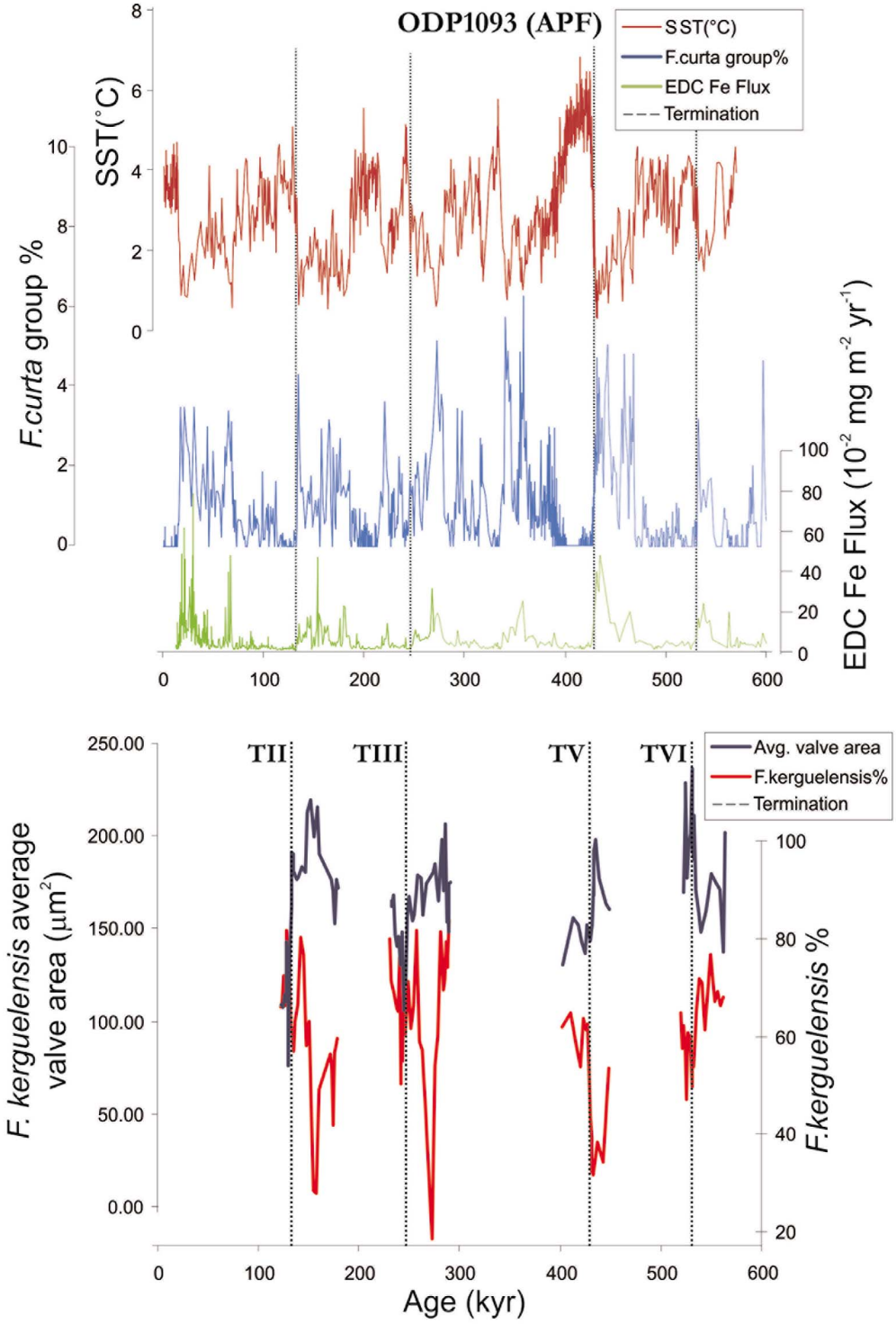

Figure 5. SST, *F. kerguelensis* and *F. curta* percentages, and *F. kerguelensis* valve area at ODP Site 1093, plus EPICA Dome C Fe flux. SST (estimated via a diatom transfer function) and diatom abundance data from *Schneider-Mor et al.* [2008]. Iron flux data for the EPICA Dome C ice core [*EPICA Community Members*, 2004; *Jouzel et al.*, 2007; *Lambert et al.*, 2008] are also shown. Vertical dashed lines mark glacial terminations.

average area values plunge to approximately 70 μm^2. During the following interglacial period, iron values remain very low and average area values fluctuate around 110 μm^2.

4.3.2. Termination III

[33] SST is slightly colder under full glacial conditions (MIS 8) than during full interglacial (MIS 7), with SST rising from ca. 2°C to a ca. 5°C maximum (Figure 5). During the

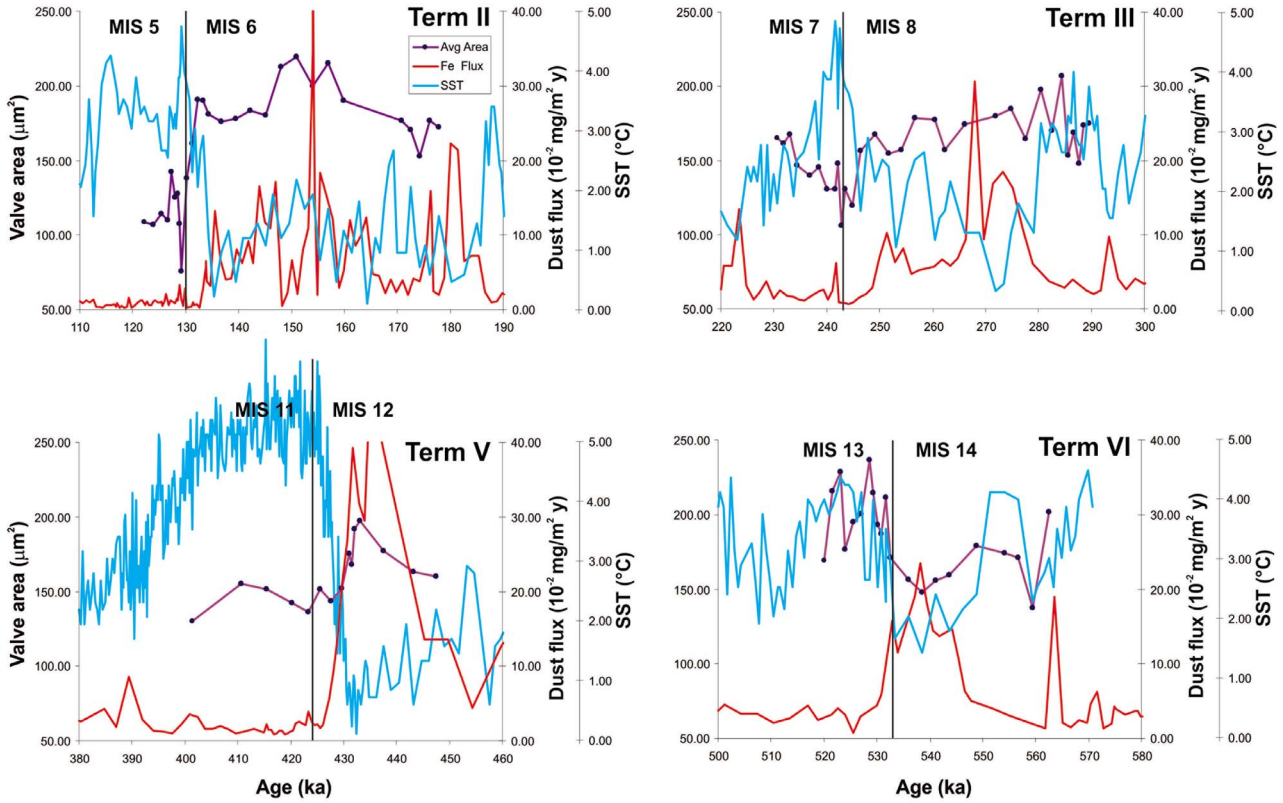

Figure 6. *F. kerguelensis* valve area and SST at ODP Site 1093, plus EPICA Dome C dust flux. The four graphs show enlargements for Terminations II, III, V, and VI for the EPICA dust flux [*EPICA Community Members*, 2004], SST at OPD Site 1093 [*Schneider-Mor et al.*, 2008], and average valve area in *F. kerguelensis* from ODP Site 1093 (this study). The right-hand scale is valid for both SST (°C) and dust flux (10^{-2} mg/m^2 y). The vertical black lines represent glacial Terminations, with their timing according to *Lisiecki and Raymo* [2005], and separate interglacial MIS (uneven numbers) from glacial marine isotopic stages (even numbers).

MIS 7 interglacial, SST decreases and fluctuates around 3°C. The correlation between SST and abundances of the sea ice–related diatom *F. curta* is clearly visible (Figure 5): during full glacial times, when temperatures are low, *F. curta* is constantly abundant and reaches peak abundances of 4%. At the onset of the Termination, the abundance of *F. curta*, and therefore sea ice concentrations, drops to almost zero. *F. kerguelensis* is constantly abundant during the whole period, with the exception of a large decrease during full glacial conditions (Figure 5). Iron concentrations are high during full glacial and positively correspond with high average area values around 170–180 μm^2 for *F. kerguelensis* (Figure 6). Once iron concentration decreases during Termination III, average area values sharply decrease to approximately 100 μm^2. During the interglacial, iron values are very low and average area values fluctuate around 150–160 μm^2.

4.3.3. Termination V

[34] SST at full glacial conditions (MIS 12) is distinctly lower than during full interglacial conditions (MIS 11), with a SST rise from ca. 0.5°C to a maximum of ca. 6.5°C (Figure 5). During the MIS 11 interglacial, SST is constant and fluctuates around 5.5°C. Over this time interval as well, there is a strong correlation between SST and amount of sea ice, as recorded by *F. curta* abundances. During full glacial times, sea ice is relatively abundant, with *F. curta* abundance peaking at 5% (Figure 5). At the onset of the Termination and during interglacial, sea ice and *F. curta* abundance levels drop to almost zero. *F. kerguelensis* displays high abundances during the whole period with an increase during interglacial (Figure 5). During full glacial, iron is high and positively corresponds with high average area valves with values of ca. 190 μm^2 for *F. kerguelensis* (Figure 6). A declining trend toward smaller interglacial valves (140–150 μm^2) is visible, corresponding to iron levels reaching almost zero.

4.3.4. Termination VI

[35] SST at full glacial conditions (MIS 14) is slightly colder than during full interglacial conditions (MIS 13), as Termination VI documents a SST rise from 1.5°C to a maximum of 4°C (Figure 5). The temperature contrast between glacial and interglacial is thus small compared to later glacial Terminations. Temperature and *F. curta* abundances are well correlated as, during full glacial times, *F. curta* reaches a peak abundance of 1.5%, indicating presence of sea ice in the proximity of the core location during this glacial period, although in lower abundance, and with a sea ice edge located south of the core location, compared to what is observed for later glacial periods (Figure 5). The cutoff value for sea ice presence is a relative abundance of 3% *F. curta*, therefore

both sea ice indicators and dust flux [*Lambert et al.*, 2008] display lower values before MIS 12 compared to later glacial intervals.

[36] At the onset of the Termination, *F. curta* abundances drop and during interglacial they remain at around zero, indicating no sea ice presence during this time interval. *F. kerguelensis* is abundant throughout this interval, with little fluctuation around 60% (Figure 5). The abundance pattern for this species is opposite to what is commonly observed, with slightly higher abundances (up to 70%) during the glacial compared to the interglacial interval (down to 50%). Its average valve area increases while iron flux decreases (Figure 6), also an opposite trend compared to what is observed at the other glacial Terminations. The highest average area measured in this study (240 μm^2) was found during the interglacial time.

5. Discussion

5.1. Iron Fertilization Experiments EIFEX and EisenEX

[37] During EIFEX all in patch and out patch stations were located within the eddy core, but the latter was not homogenous in terms of chlorophyll distribution, and mini blooms which faded away over the course of the experiment were sampled in some of the initial out stations (P. Assmy, personal communication, 2011). Moreover, some degree of diffusion between the in- and out-patch regions is to be expected.

[38] These heterogeneous conditions in the fertilized patch explain why our area values in patch and out patch differ significantly at fertilization time and before ca. day 8–12, when a significant increase in auxospore numbers is reported to occur [*Assmy et al.*, 2006], and why parallel, increasing trends from day 18 to 33 occur both inside and outside the fertilized patch. Additionally, Station 424 (the first "out patch" sample in Figure 3) can be classified as in patch/out patch, as sampled just at the border between the two areas, briefly before the Fe addition at the beginning of the EIFEX experiment.

[39] However, independent studies by P. Assmy (unpublished data, 2011) confirm that the largest (>65 μm) apical length fraction of *F. kerguelensis* was more abundant inside as compared to outside the patch, in accordance with what we observe for valve area (Figure 3).

[40] We document a trend in the iron fertilization experiments with an increase through time in valve area both inside and outside the fertilized patch. This indicates *F. kerguelensis* reacts to iron addition and to the development of a diatom bloom at the Antarctic Polar Front. This is particularly true for the EIFEX experiment, where the average valve area after 5 weeks is 40% larger than at the beginning of the fertilization.

[41] The presence of populations having, in average, larger valves inside the fertilized patch compared to the outside patch controls (Figure 3) suggests, in line with what found by *Assmy et al.* [2006] during the EIFEX experiment, that the observed increase in the number of *F. kerguelensis* auxospores upon relief from iron limitation strongly affects the population's size range.

[42] This is also in accordance with the observation that under iron-limited conditions most diatom species decrease their cell volumes by up to 50% [*Maldonado and Price*, 1996; *Marchetti and Harrison*, 2007], with the extent of this reduction being species specific. A smaller cell volume has many, very important, physiological consequences for the cell: it implies an increase of the cell surface to volume ratio, a decrease of the diffusive boundary layer thickness, a maximization of nutrient uptake rates, and a decrease in the diffusion-limited threshold for optimal growth [*Hudson and Morel*, 1990; *Pahlow et al.*, 1997]

[43] These observations lead us to turn to sedimentary records, as there are indications of increased dustiness and dust flux into the Southern Ocean and Antarctica during past glacial intervals [*Mahowald et al.*, 2006]. If this dust input increased the amount of bioavailable dissolved iron into the Southern Ocean, a large-scale "natural iron fertilization" (and relief from iron limitation) of the Southern Ocean might have occurred during these time intervals. In turn, this would have affected the average valve size in *F. kerguelensis*.

[44] There are, however, two caveats: (1) in the iron fertilization experiments (Figure 3), the trend in valve size with time inside the patch is paralleled by a similar valve size evolution outside the fertilization patch, and (2) the proposed pattern of a positive correlation of valve size with dust flux at glacial-interglacial scale (Figure 6) could as well be interpreted as a negative correlation of valve size with SST. For these reasons, the iron/dust–valve size correlation cannot serve as an indication of a causal relation between iron and valve size, and has to be considered as a working hypothesis at this stage.

5.2. Last Glacial Termination

[45] *Cortese and Gersonde* [2007] demonstrated that *F. kerguelensis* strongly fluctuates in size, with larger valves occurring at the Antarctic Polar Front during the last glacial period, and smaller valves prevailing during the Holocene interglacial. The present study was aimed at testing whether this pattern also held true at other locations in the Southern Ocean and/or at older glacial Terminations.

[46] The link between higher iron availability and larger valves in *F. kerguelensis*, which is hypothesized in the iron fertilization data, seemed to remain valid for last glacial Termination, according to our sediment data along three cores recovered from the Southern Ocean (core PS1654 from the Antarctic Polar Front, cores PS2498 and PS2499 from north of the Sub-Antarctic Front). At these different locations, the response to strongly decreased dust flux to the EDC ice core in Antarctica (and therefore presumably lower dust/Fe input to the Southern Ocean) was a strong reduction in size (from ca. 200 μm^2 during the glacial to ca. 100 μm^2 during the interglacial). Valve size remained very high during the last portion of Marine Isotope Stage (MIS) 3, through most of MIS 2, and started to decrease in concert with the decrease of dust flux between 19 and 16 kyr BP. Under MIS 1 interglacial conditions, valves seem to be larger (PS1654, ca. 150 μm^2) at the Antarctic Polar Front (APF) compared to the Sub-Antarctic Zone (ca. 100 μm^2).

[47] The correlation between valve size and dust flux (Figures 4–6), while striking, may at least partly also be a reflection of changes in wind patterns and intensity, two climate mechanism that can potentially impact diatom assemblages and valve size through their modulation of other processes in the circum-Antarctic ocean, such as upwelling

and frontal migrations. As an example of this, the trend of smaller while diverging valve sizes during Termination I and MIS 1 (Figure 3) after a prolonged time of similar valve sizes during full glacial conditions may be a consequence of diverging ocean regimes at these three core sites, probably in association with shifting circum-Antarctic wind patterns and oceanic fronts.

[48] The different baseline values in the Holocene for PS1654/ODP1093 (at the APF) are therefore probably a consequence of the different sources of iron available at the APF today (Figures 1 and 4), even under full interglacial conditions, compared to sites located further to the north in the Sub-Antarctic Zone (PS2499 and PS2498). At the APF, upwelling of deep waters [*Lefèvre and Watson*, 1999] and melting icebergs/sea ice [*Raiswell et al.*, 2006; *Smith et al.*, 2007; *Geibert et al.*, 2010] may provide sources of bioavailable iron that fuel slightly larger valve sizes in *F. kerguelensis*, even in the absence of the dominant eolian source. None of those additional iron sources seem to play an important role in the Sub-Antarctic Zone.

[49] In order to test whether other sources of iron, in addition to eolian dust, might at times have become important close to the Antarctic Polar Front in the Southern Ocean over last 35 ka, we compared (Figure 4) our valve area record for last glacial Termination to records of ice-rafted debris [*Kanfoush et al.*, 2002], a proxy for iron sourced from melting icebergs, and Th-corrected opal flux [*Anderson et al.*, 2009], a proxy for iron sourced from upwelling of deep waters.

[50] However, overall in the Atlantic Southern Ocean IRD deposition is important only during glacials [*Diekmann et al.*, 2003] and thus acts in the same direction as the eolian dust deposition. In fact, more than 90% of the IRD signal recorded by *Kanfoush et al.* [2002] was later identified to represent tephra particles transported by sea ice from the South Sandwich Island volcanic arc, and not by icebergs from the Antarctic continent [*Nielsen et al.*, 2007]. It is highly unlikely that the tephra particles, when falling through the water column after sea ice melt, will have an effect on the micronutrient concentration in surface waters.

[51] More likely sources besides the eolian input [see *Ridgwell and Watson*, 2002] are the advection of Fe-enriched deep water by intensified upwelling and icebergs, as proposed by *Abelmann et al.* [2006] for Termination I in the study area. Such mechanisms of Fe deposition, although not exceeding the effect of dust, may explain the prolonged decline of the F. *kerguelensis* valve size at glacial terminations.

[52] Increased Th-corrected opal flux (used as a proxy for increased advection of the nutrient silicon by upwelling) is restricted to the 10–17 ka time window (i.e., at the glacial Termination). In contrast, strong upwelling of deep and nutrient-rich waters during glacials is not supported by nutrient proxies [*Sigman et al.*, 2010]. The potential of Fe deposition by iceberg melting was highlighted by *Smith et al.* [2007].

[53] We can draw the following conclusions from these observations: (1) Iron deposition in surface waters by upwelling is negligible during the glacial (and thus cannot have an influence on glacial valve size), but may play a role during the increased upwelling of nutrient-rich water at glacial terminations; (2) a second source of Fe may be iceberg melting, preferentially at terminations; and (3) both additional sources (upwelling and icebergs) do not cause a valve size effect that exceeds the one caused by dust deposition during glacials. The valve area data set for Termination I also allowed us to test whether there was a change in population structure between MIS 1 to MIS 2, and what the possible biological reasons for this may have been. There is a certain degree of positive correlation between valve size and standard deviation, albeit variable between glacial Terminations/sites (Figure S3a), with a maximum correlation value ($r^2 = 0.49$) observed for ODP Site 1093, with all previous glacial Termination data grouped together. This positive correlation might suggest a size spectrum shift from glacial to interglacial times, with a broader size range during glacial intervals.

[54] The histograms for all valve area measurements from MIS1 and MIS2 (Figures S3b and S3c), both all grouped together and split core by core (PS2499, PS2498, PS1654), albeit not easy to compare directly, as they are based on a different number of observations, seem to indicate how (1) both distributions are skewed toward low values, and this is more extreme for the MIS1 interglacial population, and (2) the size range is broader for the glacial population, particularly for values from ca. 200 to 400 μm^2, which are relatively underrepresented in the interglacial population. Both these observations seem to hold true as well once the data are split by core.

[55] These data may indicate how *F. kerguelensis* populations resorted more frequently to auxospore formation during glacial (MIS2) compared to interglacial (MIS1) times, in line with what observed during iron fertilization experiments in the modern ocean, where auxospore abundances increase in the fertilized patch [*Assmy et al.*, 2006]. Furthermore, the prevailing conditions of limited Fe availability during interglacial times may have affected this diatom's life cycle, resulting in the production of auxospores of smaller size, thus constraining the population within a narrower cell size range.

[56] Our main hypothesis is therefore that the size increase following iron addition (either in fertilization experiments or glacial times) is related to an increase in the importance of the auxospore stage in this diatom's life cycle. This can be represented by either an increase in their total number, as demonstrated by *Assmy et al.* [2006] for iron fertilization experiments, and/or in the auxospore area itself. For our glacial Termination I data, the result of these processes is represented by a shift in size spectra for the whole population (Figure S3b).

[57] As also suggested by *Assmy et al.* [2006], another biological process may also have played an important role in shaping the population structure: selective predation of the more fragile (compared to the vegetative cell) auxospore stage during interglacial compared to glacial intervals. Under this scenario, a specific predator (maybe present in higher numbers during warmer intervals?) would have been more efficient in removing the ca. 250 to 400 μm^2 size fraction during interglacial compared to glacial times.

[58] However, many additional complexities, particularly behind predation and export mechanisms, suggest exerting caution when attempting a direct interpretation of the size structure of the populations. Such interpretation is probably best left to a more in-depth treatment of additional data from culturing and ecosystem modeling, which are currently being

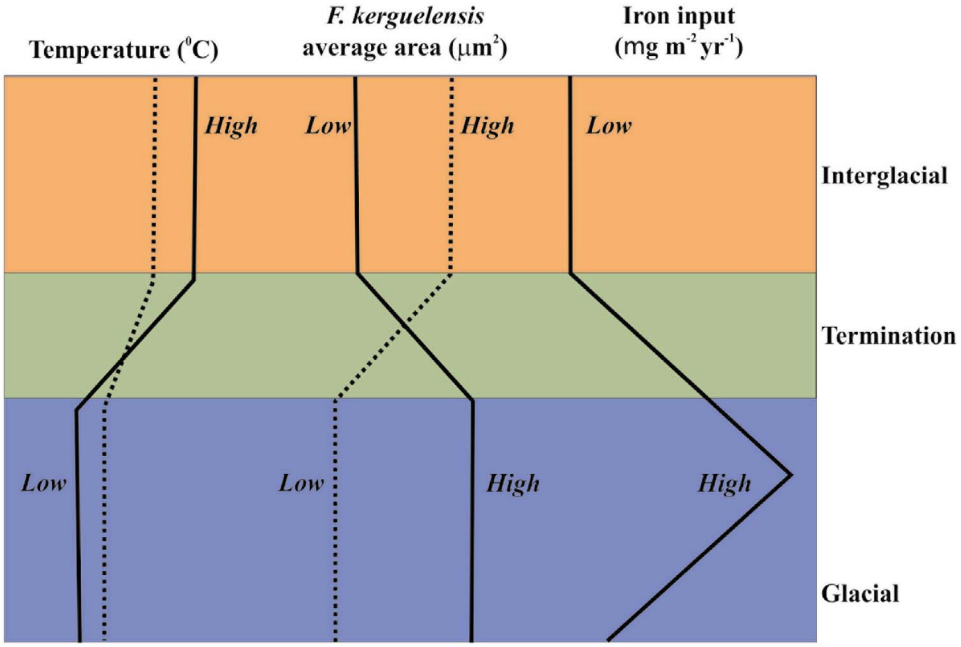

Figure 7. Schematic illustration of the correlation between temperature, average valve area, and iron flux through several glacial Terminations. Results for Terminations I, II, III, and V are represented by solid lines, and dashed lines mark results for Termination VI.

collected by fellow researchers in an underway collaborative study between AWI and the Zoological Station "Anton Dohrn," Naples.

5.3. Previous Terminations

[59] We then checked how *F. kerguelensis* fared at the Antarctic Polar Front through previous glacial Terminations, by producing records of its average valve area variability through the last 550 ka at ODP Site 1093. Maximum average valve areas for this diatom were indeed found under glacial conditions, while smaller valves occurred during interglacial times (Figure 6). During full glacial times the valve size was about 200 μm^2 on average, and therefore ca. twice as large as under interglacial conditions. This pattern was observed at Termination II, Termination III and Termination V, and thus matched well the previously observed pattern for Termination I. However, the time interval around Termination VI shows an inverse relationship between valve size and glacial/interglacial conditions (Figures 6 and 7): *F. kerguelensis* valves were larger during MIS 13 (interglacial) and smaller during MIS 14 (glacial). The largest valve areas measured in this study (up to 240 μm^2) were found during MIS 13.

[60] In order to better understand the paleoenvironmental significance of the observed size changes in *F. kerguelensis*, we tested the link between them and several proxy record time series, including sea ice temperature, sea ice extent, eolian input, as well as major ecosystem shifts within diatoms. The diatom *F. kerguelensis* is constantly abundant through time in the Southern Ocean, with slightly higher relative abundances during interglacial times. In order to test the effect of changes in iron availability and relief from iron limitation in the Southern Ocean on the valve size of *F. kerguelensis*, we compared our sediment core records for size variability over several glacial-interglacial transitions to a regional record of dust input and flux stored in an Antarctic ice core. The EPICA Dome C ice core from East Antarctica provides highly resolved records of atmospheric parameters over last 800,000 years, including a significant increase of iron in glacial compared to interglacial periods [*Wolff et al.*, 2006]. This proxy record of iron flux shows increased iron input to the Southern Ocean during glacial conditions, and thus potentially a strong linkage between higher valves areas averages of *F. kerguelensis* during this period, and higher dust/iron concentrations.

[61] Our valve area data for Termination VI indicate smaller valves during full glacial and an increase to larger valves during full interglacial conditions (i.e., a pattern opposite to what observed at the other, later, glacial Terminations).

[62] In this respect, it is interesting to note how at this glacial Termination both the oceanic SST and atmospheric CO_2 concentration contrast between full glacial and interglacial conditions was strongly reduced compared to later glacial Terminations. In fact, the CO_2 record from the EPICA Dome C core [*Siegenthaler et al.*, 2005] displays the partial pressure of atmospheric CO_2 oscillating between 260 and 180 ppm before 430 ka, a range that is almost 30% smaller than that of the last four glacial cycles. *Martínez-Garcia et al.* [2009] suggest that such a change in the amplitude of the CO_2 cycles was most likely driven by physical processes, and related to changes in Antarctic sea ice extent, surface water stratification, and westerly winds position. Changes in these three processes will have strong consequences on both diatoms and the whole Southern Ocean ecosystem, thus signifying different boundary conditions and response to glacial Terminations in the Southern Ocean during Termination VI and older, compared to younger time intervals.

[63] Indications of substantial diatom assemblage differences are noticeable when comparing Termination VI floral records to those representative of younger glacial Terminations: lower relative abundances of *Chaetoceros* spp. (ca. 5% versus 30%, indicating a very different diatom assemblage and possibly lower competition for dissolved nutrients in *F. kerguelensis*) and lower relative abundances of *Fragilariopsis obliquecostata* and *F. curta* (indicating lower summer and winter sea ice coverage). On longer timescales, shifts in diatom assemblage composition have been demonstrated to play an important role in the geological history of biogenic silica burial in the Southern Ocean over the past 3–4 million years [*Cortese and Gersonde*, 2008]. These floral shifts strongly affected the export efficiency, and ultimately helped in establishing the Antarctic Polar Front as the main site for burial of biogenic silica in the World Ocean, with *F. kerguelensis* as the prime exporter. At the suborbital scale of interest here, relative abundance shifts may have as well contributed to a different functioning of the Southern Ocean ecosystem.

[64] An additional line of evidence for an anomalous behavior during Termination VI comes from *F. kerguelensis* itself: as mentioned above, the correlation of valve size to SST is usually negative (higher SSTs correspond to smaller valves and vice versa), while for Termination VI the correlation is positive (higher SSTs correspond to larger valves). However, at this Termination, *F. kerguelensis* relative abundances display a peculiar pattern, as this species is (opposite to what is commonly observed in the Southern Ocean) more abundant during the glacial MIS 14 compared to the interglacial MIS 13 (Figure 5). As this species is usually a warm water indicator in the Southern Ocean and is very abundant in this area, the observed pattern suggests that SST is not the only control on the abundance and size of this species at Termination VI.

[65] In our study, with the exception of Termination VI, there is a negative correlation between valve area and relative abundances in *F. kerguelensis*: larger mean valve areas are observed when the relative abundance of this species is lower (during glacial intervals). This result is the opposite of what is observed in a recent biometric investigation of *F. kerguelensis* [*Crosta*, 2009]. In a study of Holocene samples from sediment core MD03–2601 (Antarctic Continental Shelf off Adélie Land, East Antarctica), *Crosta* [2009] found this species to be bigger and more abundant during the warmer mid-Holocene period and smaller and less abundant during the colder late Holocene period, that is, a positive correlation between valve size and relative abundance in *F. kerguelensis*. Two considerations allow reconciliation of these seemingly conflicting lines of evidence:

[66] 1. Holocene boundary conditions are different from those prevailing during glacial times and glacial Terminations. Therefore, the changes in size observed in these two studies (one based on an interglacial record, the present study looking at changes between glacial, glacial Terminations, and interglacials) may have had different controls and significance.

[67] 2. We concur with *Crosta* [2009] that the strongest control on size in *F. kerguelensis* is most likely linked to favorable environmental/paleobiological conditions for this species in the environment where it is observed. *Crosta* [2009] argues that the observed positive size/abundance relationship is linked to the fact that the core location stands today at the lower ecologic limit for *F. kerguelensis*. At the Antarctic continental shelf location, where iron limitation is not an issue, more adequate environmental conditions for *F. kerguelensis* (warmer, less icy) allowed restoration of bigger initial cells and overall bigger average size for the entire populations. In our study, monitoring *F. kerguelensis* in a prime iron-depleted area of the ocean (where ecological conditions in terms of SST and sea ice are far from the limit for this species, and are actually close to optimal), the SST control on the valve size of this species may have played a subordinate role compared to the availability of iron. These different controls might have given rise to the negative relationship observed in this study between valve size and relative abundance at the Antarctic Polar Front, with lower SSTs (but higher iron content) during glacial times representing "favorable conditions" for larger *F. kerguelensis* valves at this location.

6. Conclusions

[68] 1. Two iron fertilization experiments suggest the possibility that the valve area of *Fragilariopsis kerguelensis* increases in water samples containing elevated iron concentrations. There is an offset of ca. 20–30 μm^2 between the in- and out-patch time series, with the in-patch populations being consistently larger than the out-patch populations, most likely a result of the increased number of auxospores in the in-patch samples.

[69] 2. The study of last glacial Termination at three different locations in the Southern Ocean (core PS1654 from the Antarctic Polar Front, cores PS2498 and PS2499 from the Sub-Antarctic Zone) provides strong evidence for the occurrence of larger average valve areas of *F. kerguelensis* during the glacial MIS 2 compared to the interglacial MIS 1. A synchronous drop in dust flux during Termination I recorded in the EDC ice core opens the possibility that decreased dust-derived Fe flux to the Southern Ocean played a role in establishing predominantly smaller valve sizes.

[70] 3. The analysis of valve size variability at the Antarctic Polar Front (ODP Site 1093) over several past glacial Terminations, spanning the shift from full glacial to full interglacial conditions, revealed how average valve size seems to be directly correlated to increased input of eolian dust to the Southern Ocean, and inversely correlated to Sea Surface Temperature.

[71] 4. This correlation does not seem to be valid for glacial Termination VI, where size appears to be inversely correlated to dust input. Anomalous patterns in species composition (for *Chaetoceros* spp., *F. obliquecostata*, and *F. curta*), relative abundances of *F. kerguelensis*, sea ice extent, SST, and CO_2 conditions are all possible explanations for the deviation from the expected pattern of larger valve size during glacial compared to interglacial times.

[72] 5. SST can still prevail over iron/dust input in controlling average valve size of *F. kerguelensis* in environments, such as those prevailing during the Holocene close to the Wilkes' Land Antarctic coast, where the SST conditions are very close to the lower ecological limit for this species.

[73] 6. At this stage, the linkage between iron availability, flux of dust to the surface ocean around Antarctica, and valve area in *F. kerguelensis* (albeit very likely given the impact, well documented in literature, Fe limitation has on diatom size) remains hypothetical, and has yet to be confirmed by further studies and more in-depth statistical examination of these and similar data sets. As an example, promising inroads in establishing causal links between other morphometric characters (e.g., length-normalized width) and environmental conditions have been performed by *Marchetti and Cassar* [2009], based on the previously published version of this data set [*Cortese and Gersonde*, 2007], including only surface sediment and Termination I data from one locality.

[74] **Acknowledgments.** Research was funded by the New Zealand Foundation for Research, Science, and Technology (FRST) program Global Change Through Time and by the Research Center Ocean Margins, Bremen, Germany. The iron fertilization experiments samples were kindly provided by Philipp Assmy (AWI, Bremerhaven). Laboratory assistance and slide preparation by Ute Bock (AWI, Bremerhaven) is gratefully acknowledged. Four anonymous reviewers are thanked for providing excellent suggestions, which greatly improved the quality of the final manuscript.

References

Abelmann, A., R. Gersonde, G. Cortese, G. Kuhn, and V. Smetacek (2006), Extensive phytoplankton blooms in the Atlantic sector of the glacial Southern Ocean, *Paleoceanography*, *21*, PA1013, doi:10.1029/2005PA001199.

Anderson, R. F., S. Ali, L. I. Bradtmiller, S. H. H. Nielsen, M. Q. Fleisher, B. E. Anderson, and L. H. Burckle (2009), Wind-driven upwelling in the Southern Ocean and the deglacial rise in atmospheric CO_2, *Science*, *323*(5920), 1443–1448, doi:10.1126/science.1167441.

Assmy, P., J. Henjes, V. Smetacek, and M. Montresor (2006), Auxospore formation by the silica-sinking, oceanic diatom *Fragilariopsis kerguelensis* (*Bacillariophyceae*), *J. Phycol.*, *42*, 1002–1006, doi:10.1111/j.1529-8817.2006.00260.x.

Belkin, I. M., and A. L. Gordon (1996), Southern Ocean fronts from the Greenwich meridian to Tasmania, *J. Geophys. Res.*, *101*(C2), 3675–3696, doi:10.1029/95JC02750.

Boyd, P. W., et al. (2000), A mesoscale phytoplankton bloom in the polar Southern Ocean stimulated by iron fertilization, *Nature*, *407*, 695–702, doi:10.1038/35037500.

Chepurnov, V. A., D. G. Mann, K. Sabbe, and W. Vyverman (2004), Experimental studies on sexual reproduction in diatoms, *Int. Rev. Cytol.*, *237*, 91–154, doi:10.1016/S0074-7696(04)37003-8.

Coale, K. H., et al. (1996), A massive phytoplankton bloom induced by an ecosystem-scale iron fertilization experiment in the equatorial Pacific Ocean, *Nature*, *383*, 495–501, doi:10.1038/383495a0.

Cortese, G., and R. Gersonde (2007), Morphometric variability in the diatom *Fragilariopsis kerguelensis*: Implications for Southern Ocean paleoceanography, *Earth Planet. Sci. Lett.*, *257*, 526–544, doi:10.1016/j.epsl.2007.03.021.

Cortese, G., and R. Gersonde (2008), Plio/Pleistocene changes in the main biogenic silica carrier in the Southern Ocean, Atlantic Sector, *Mar. Geol.*, *252*, 100–110, doi:10.1016/j.margeo.2008.03.015.

Crosta, X. (2009), Holocene size variations in two diatom species off East Antarctica: Productivity vs environmental conditions, *Deep Sea Res., Part I*, *56*, 1983–1993, doi:10.1016/j.dsr.2009.06.009.

de Baar, H. J. W., A. G. J. Buma, R. F. Nolting, G. C. Cadée, G. Jacques, and P. J. Tréguer (1990), On iron limitation of the Southern Ocean: Experimental observations in the Weddell and Scotia Seas, *Mar. Ecol. Prog. Ser.*, *65*, 105–122, doi:10.3354/meps065105.

De La Rocha, C. L., D. A. Hutchins, M. A. Brzezinski, and Y. Zhang (2000), Effects of iron and zinc deficiency on elemental composition and silica production by diatoms, *Mar. Ecol. Prog. Ser.*, *195*, 71–79, doi:10.3354/meps195071.

Diekmann, B., D. K. Fütterer, H. Grobe, C. D. Hillenbrand, G. Kuhn, K. Michels, R. Petschick, and M. Pirrung (2003), Terrigenous sediment supply in the polar to temperature South Atlantic: Land-ocean links of environmental changes during the Late Quaternary, in *The South Atlantic in the Late Quaternary: Reconstruction of Material Budgets and Current Systems*, edited by G. Wefer et al., pp. 375–399, Springer, Berlin.

EPICA Community Members (2004), Eight glacial cycles from Antarctic ice core, *Nature*, *429*, 623–628, doi:10.1038/nature02599.

Falkowski, P. G., R. T. Barber, and V. Smetacek (1998), Biogeochemical controls and feedbacks on ocean primary production, *Science*, *281*(5374), 200–206, doi:10.1126/science.281.5374.200.

Fenner, J., H.-J. Schrader, and H. Wienigk (1976), Diatom phytoplankton studies in the southern Pacific Ocean, composition and correlation to the Antarctic Convergence and its paleoecological significance, *Initial Rep. Deep Sea Drill. Proj.*, *35*, 757–813, doi:10.2973/dsdp.proc.35.app3.1976.

Geibert, W., et al. (2010), High productivity in an ice melting hot spot at the eastern boundary of the Weddell Gyre, *Global Biogeochem. Cycles*, *24*, GB3007, doi:10.1029/2009GB003657.

Gersonde, R., and U. Zielinski (2000), The reconstruction of late Quaternary Antarctic sea-ice distribution—The use of diatoms as a proxy for sea-ice, *Palaeogeogr. Palaeoclimatol. Palaeoecol.*, *162*, 263–286, doi:10.1016/S0031-0182(00)00131-0.

Hodell, D. A., R. Gersonde, and P. Blum (2002), Leg 177 synthesis: Insights into Southern Ocean paleoceanography on tectonic to millennial timescales [online], *Proc. Ocean Drill. Program Sci. Results*, *177*. [Available at http://www-odp.tamu.edu/publications/177_SR/synth/synth.htm.]

Hudson, R. J. M., and F. M. M. Morel (1990), Iron transport in marine phytoplankton: Kinetics of cellular and medium coordination reactions, *Limnol. Oceanogr.*, *35*, 1002–1020, doi:10.4319/lo.1990.35.5.1002.

Hutchins, D. A., and K. W. Bruland (1998), Iron-limited diatom growth and Si:N uptake ratios in a coastal upwelling regime, *Nature*, *393*, 561–564, doi:10.1038/31203.

Jouzel, J., et al. (2007), Orbital and millennial Antarctic climate variability over the past 800,000 years, *Science*, *317*(5839), 793–796, doi:10.1126/science.1141038.

Kanfoush, S. L., D. A. Hodell, C. D. Charles, T. R. Janecek, and F. R. Rack (2002), Comparison of ice-rafted debris and physical properties in ODP Site 1094 (South Atlantic) with the Vostok ice core over the last four climatic cycles, *Palaeogeogr. Palaeoclimatol. Palaeoecol.*, *182*, 329–349, doi:10.1016/S0031-0182(01)00502-8.

Lambert, F., B. Delmonte, J. R. Petit, M. Bigler, P. R. Kaufmann, M. A. Hutterli, T. F. Stocker, U. Ruth, J. P. Steffensen, and V. Maggi (2008), Dust-climate couplings over the past 800,000 years from the EPICA Dome C ice core, *Nature*, *452*, 616–619, doi:10.1038/nature06763.

Lefèvre, N., and A. J. Watson (1999), Modeling the geochemical cycle of iron in the oceans and its impact on atmospheric CO_2 concentrations, *Global Biogeochem. Cycles*, *13*, 727–736, doi:10.1029/1999GB900034.

Lisiecki, L. E., and M. E. Raymo (2005), A Pliocene-Pleistocene stack of 57 globally distributed benthic $\delta^{18}O$ records, *Paleoceanography*, *20*, PA1003, doi:10.1029/2004PA001071.

Mahowald, N. M., D. R. Muhs, S. Levis, P. J. Rasch, M. Yoshioka, C. S. Zender, and C. Luo (2006), Change in atmospheric mineral aerosols in response to climate: Last glacial period, preindustrial, modern, and doubled carbon dioxide climates, *J. Geophys. Res.*, *111*, D10202, doi:10.1029/2005JD006653.

Maldonado, M. T., and N. M. Price (1996), Influence of N substrate on Fe requirements of marine centric diatoms, *Mar. Ecol. Prog. Ser.*, *141*, 161–172, doi:10.3354/meps141161.

Mann, D. G. (1999), The species concept in diatoms, *Phycologia*, *38*, 437–495, doi:10.2216/i0031-8884-38-6-437.1.

Marchetti, A., and N. Cassar (2009), Diatom elemental and morphological changes in response to iron limitation: A brief review with potential paleoceanographic applications, *Geobiology*, *7*, 419–431, doi:10.1111/j.1472-4669.2009.00207.x.

Marchetti, A., and P. J. Harrison (2007), Coupled changes in the cell morphology and the elemental (C, N and Si) composition of the pennate diatom *Pseudo-nitzschia* due to iron deficiency, *Limnol. Oceanogr.*, *52*, 2270–2284, doi:10.4319/lo.2007.52.5.2270.

Martin, J. H., and S. E. Fitzwater (1988), Iron deficiency limits phytoplankton growth in the north-east Pacific subarctic, *Nature*, *331*, 341–343, doi:10.1038/331341a0.

Martin, J. H., R. M. Gordon, and S. E. Fitzwater (1990), Iron in Antarctic waters, *Nature*, *345*, 156–158, doi:10.1038/345156a0.

Martin, J. H., et al. (1994), Testing the iron hypothesis in ecosystems of the equatorial Pacific Ocean, *Nature*, *371*, 123–129, doi:10.1038/371123a0.

Martínez-Garcia, A., A. Rosell-Melé, W. Geibert, R. Gersonde, P. Masqué, V. Gaspari, and C. Barbante (2009), Links between iron supply, marine productivity, sea surface temperature, and CO_2 over the last 1.1 Ma, *Paleoceanography*, *24*, PA1207, doi:10.1029/2008PA001657.

Nielsen, S. H. H., D. A. Hodell, G. Kamenov, T. Guilderson, and M. R. Perfit (2007), Origin and significance of ice-rafted detritus in the Atlantic sector of the Southern Ocean, *Geochem. Geophys. Geosyst.*, *8*, Q12005, doi:10.1029/2007GC001618.

Pahlow, M., U. Riebesell, and D. A. Wolf-Gladrow (1997), Impact of cell shape and chain formation on nutrient acquisition by marine diatoms, *Limnol. Oceanogr.*, *42*, 1660–1672, doi:10.4319/lo.1997.42.8.1660.

Paillard, D., L. Labeyrie, and P. Yiou (1996), Macintosh program performs time-series analysis, *Eos Trans. AGU*, *77*(39), 379, doi:10.1029/96EO00259.

Parrenin, F., et al. (2007), The EDC3 chronology for the EPICA Dome C ice core, *Clim. Past*, *3*, 485–497, doi:10.5194/cp-3-485-2007.

Raiswell, R., M. Tranter, L. G. Benning, M. Siegert, R. De'ath, P. Huybrechts, and T. Payne (2006), Contributions from glacially derived sediment to the global iron (oxyhydr)oxide cycle: Implications for iron delivery to the oceans, *Geochim. Cosmochim. Acta*, *70*, 2765–2780, doi:10.1016/j.gca.2005.12.027.

Ridgwell, A. J., and A. J. Watson (2002), Feedback between aeolian dust, climate, and atmospheric CO_2 in glacial time, *Paleoceanography*, *17*(4), 1059, doi:10.1029/2001PA000729.

Sarmiento, J. L., N. Gruber, M. A. Brzezinski, and J. P. Dunne (2004), High-latitude controls of thermocline nutrients and low latitude biological productivity, *Nature*, *427*, 56–60, doi:10.1038/nature02127.

Schneider-Mor, A., R. Yam, C. Bianchi, M. Kunz-Pirrung, R. Gersonde, and A. Shemesh (2008), Nutrient regime at the siliceous belt of the Atlantic sector of the Southern Ocean during the past 660 ka, *Paleoceanography*, *23*, PA3217, doi:10.1029/2007PA001466.

Siegenthaler, U., et al. (2005), Stable carbon cycle–climate relationship during the late Pleistocene, *Science*, *310*(5752), 1313–1317, doi:10.1126/science.1120130.

Sigman, D. M., M. P. Hain, and G. H. Haug (2010), The polar ocean and glacial cycles in atmospheric CO_2 concentration, *Nature*, *466*, 47–55, doi:10.1038/nature09149.

Smetacek, V. (2001), EisenEx: International team conducts iron experiment in Southern Ocean, *U.S. JGOFS News*, *11*(1), 14.

Smetacek, V., U. Bathmann, and E. Helmke (Eds.) (2005), The expeditions ANTARKTIS XXI/3-4-5 of the research vessel *Polarstern* in 2004, *Ber. Polarforsch. Meeresforsch*. *500*, 302 pp., Alfred Wegener Inst. for Polar and Mar. Res., Bremerhaven, Germany, hdl:10013/epic.10505.d001.

Smith, K. L., Jr., B. H. Robison, J. J. Helly, R. S. Kaufmann, H. A. Ruhl, T. J. Shaw, B. S. Twining, and M. Vernet (2007), Free-drifting icebergs: Hot spots of chemical and biological enrichment in the Weddell Sea, *Science*, *317*(5837), 478–482 doi:10.1126/science.1142834.

Takeda, S. (1998), Influence of iron availability on nutrient consumption ratio of diatoms in oceanic waters, *Nature*, *393*, 774–777, doi:10.1038/31674.

Timmermans, K. R., B. van der Wagt, and H. J. W. de Baar (2004), Growth rates, half saturation constants, and silicate, nitrate, and phosphate depletion in relation to iron availability of four large, open-ocean diatoms from the Southern Ocean, *Limnol. Oceanogr.*, *49*, 2141–2151, doi:10.4319/lo.2004.49.6.2141.

Wolff, E. W., et al. (2006), Southern Ocean sea-ice extent, productivity and iron flux over the past eight glacial cycles, *Nature*, *440*, 491–496, doi:10.1038/nature04614.

G. Cortese, Department of Paleontology, GNS Science, 1 Fairway Dr., PO Box 30 368, Lower Hutt 5040, New Zealand. (g.cortese@gns.cri.nz)

R. Gersonde, Geosciences Division, Alfred Wegener Institute for Polar and Marine Research, Columbusstrasse, PO Box 120161, Bremerhaven D-27515, Germany. (rainer.gersonde@awi.de)

K. Maschner, German Oceanographic Museum, Katharinenberg 14-60, Stralsund D-18439, Germany. (katharina.maschner@meeresmuseum.de)

P. Medley, Cooperative Institute for Research in Environmental Sciences, University of Colorado at Boulder, 216 UCB, Boulder, CO 80309-0216, USA. (pamela.medley@colorado.edu)